Supplementary Figures

A repeat sequence domain of the ring-exported protein-1 of *Plasmodium falciparum* controls export machinery architecture and virulence protein trafficking

Emma McHugh[1], Steven Batinovic[1], Eric Hanssen[1,2], Paul J. McMillan[1,3], Shannon Kenny[1], Michael D.W. Griffin[1], Simon Crawford[4], Katharine R. Trenholme[5], Donald L. Gardiner[5], Matthew W. A. Dixon[1#], and Leann Tilley[1#*]

[1]Department of Biochemistry and Molecular Biology, [2]Advanced Microscopy Facility, and [3]Biological Optical Microscopy Platform, Bio21 Molecular Science and Biotechnology Institute, and [4]School of BioSciences, University of Melbourne, Parkville, VIC 3010, Australia, [5]Infectious Diseases Division, Queensland Institute of Medical Research, 300 Herston Rd, Herston, QLD 4006, Australia

*For correspondence: E-mail: ltilley@unimelb.edu.au

#These authors had equal contribution

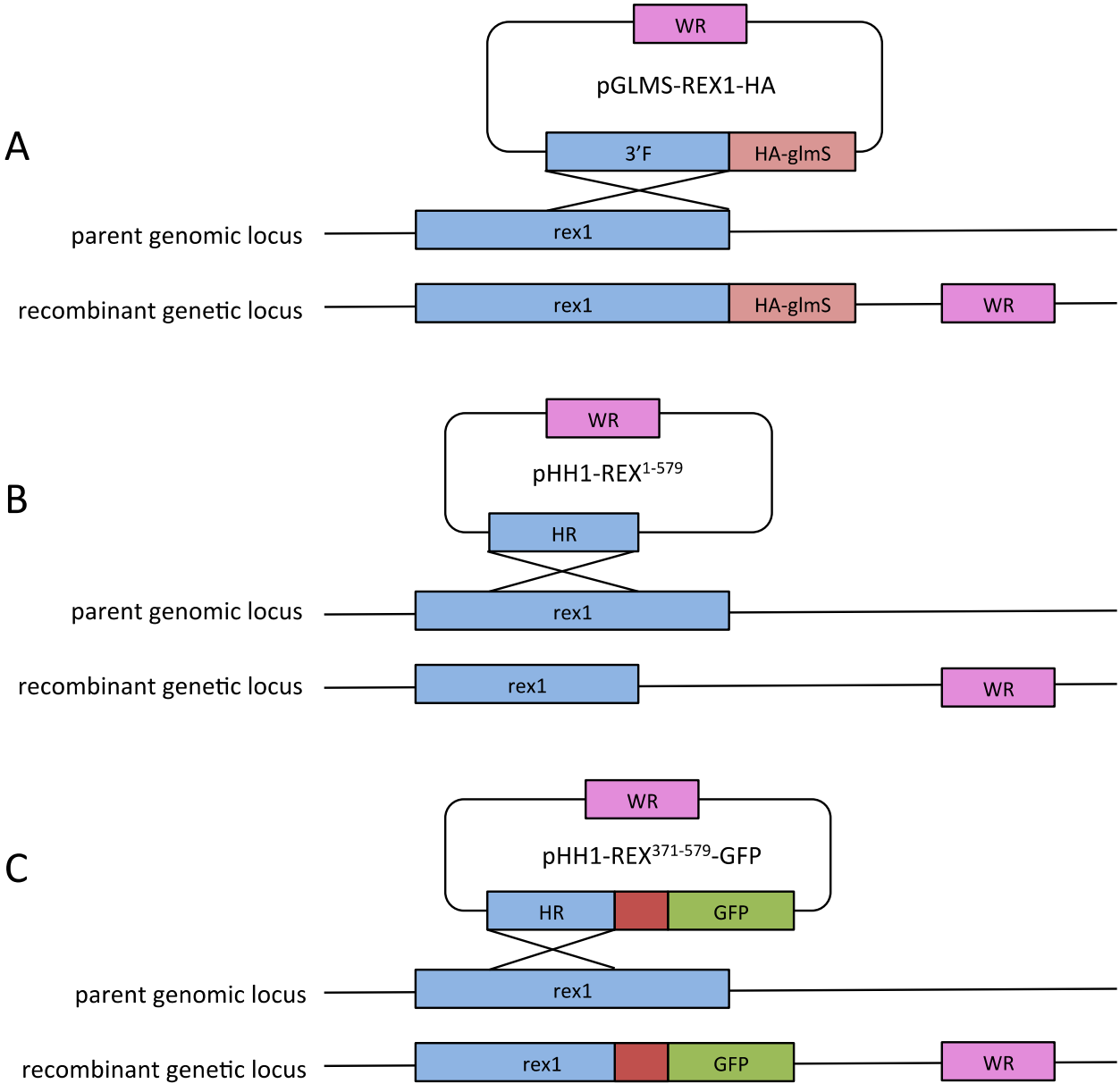

Fig. S1. Schematic representation of strategy used to generate transfected parasites. A. REX1-HA-glmS, 3'F = 3' flank. B. REX1$^{1-579}$, HR = homologous region. C. REX1$^{(\Delta 371-579)}$-GFP.

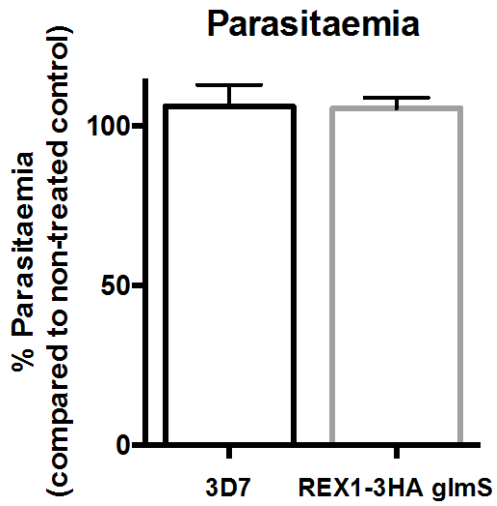

Fig. S2. Analysis of the growth of 3D7 and REX1-KD parasites in the presence and absence of GlcN. Parasites were synchronized to a 2 h window and were treated, or not, with GlcN at 24 h post-invasion. 48 h later the infected RBCs were labelled with SYTO61 and parasitemia levels were determined using flow cytometry. Results are presented as a percentage of untreated control ± S.D.

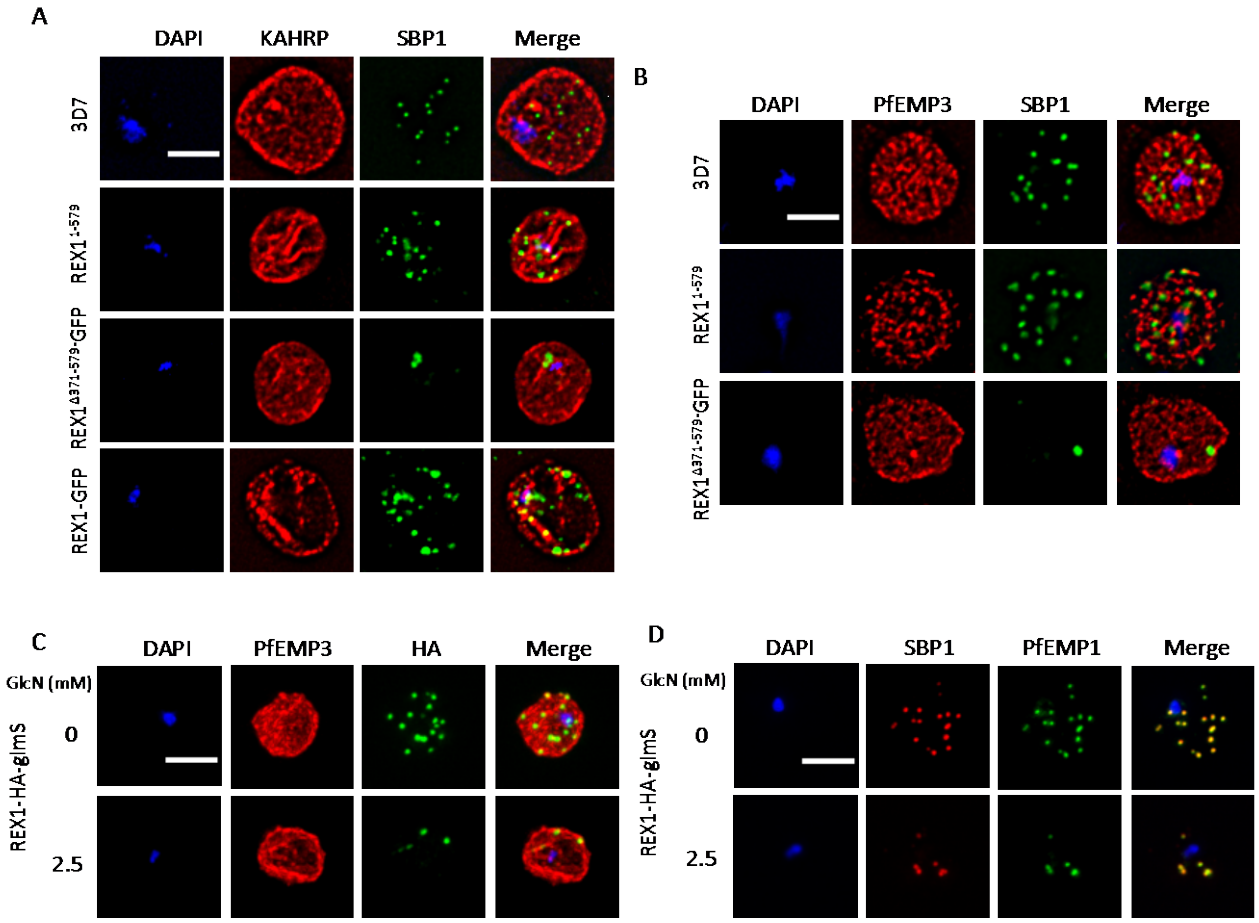

Fig. S3. Immunofluorescence microscopy of KAHRP, PfEMP3 and PfEMP1. Immunofluorescence microscopy was performed on acetone- (A,B) or paraformaldehyde-(C,D) fixed infected RBCs probed with anti-KAHRP, anti-PfEMP3, anti-HA, anti-ATS or anti-SBP1 antibodies. Nuclei are stained with DAPI (blue). Scale bar = 3 μm.

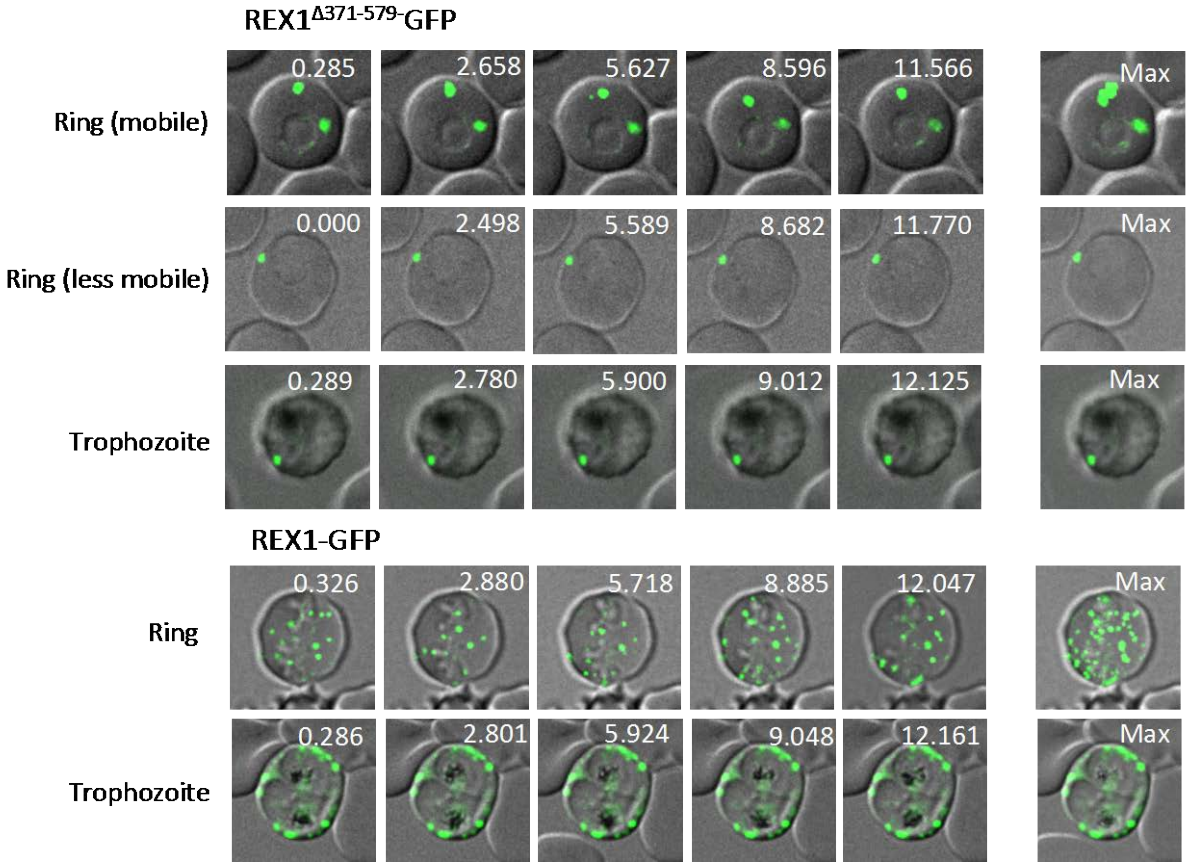

Fig. S4. Live cell imaging of REX1-GFP and REX1$^{(\Delta 371–579)}$-GFP ring- and trophozoite-infected RBCs. Top panel: A ring stage REX1$^{(\Delta 371–579)}$-GFP-infected RBC with mobile Maurer's clefts. Second panel: A REX1$^{(\Delta 371–579)}$-GFP ring stage parasite with a Maurer's cleft with limited mobility. Third panel: Immobilized Maurer's cleft from a REX1$^{(\Delta 371–579)}$-GFP trophozoite stage parasite. Forth panel: Ring stage REX1-GFP parasites with mobile Maurer's clefts. Fifth panel: Immobilized Maurer's clefts in a trophozoite stage REX1-GFP parasite. Maximum projections of each of the series of five time points are presented on the far right. Times from beginning of acquisition are stamped on each image in seconds.

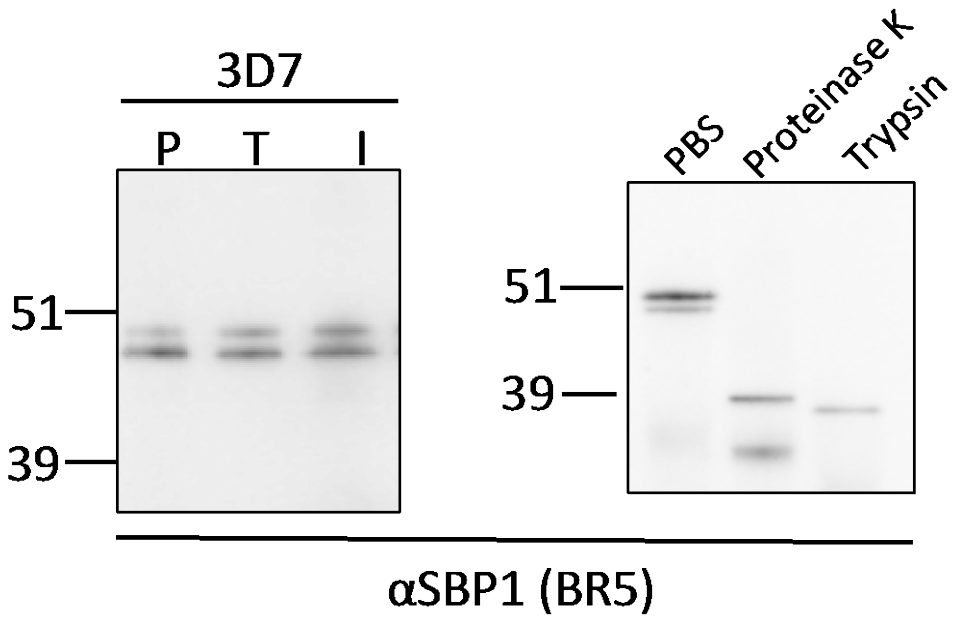

Fig. S5. Control to monitor integrity of infected RBCs during trypsin digestion. Left panel: 3D7 parasites were treated with PBS (P), PBS and trypsin (T) or PBS, trypsin and soybean trypsin inhibitor (I). The reaction was stopped with soybean trypsin inhibitor and the cells were permeabilized with EqtII to release hemoglobin. The samples were subjected to SDS-PAGE and Western blotting. Right panel: 3D7 parasites were permeabilized with EqtII and treated with either PBS, proteinase K or trypsin. Proteins were precipitated with trichloroacetic acid and subjected to SDS-PAGE and Western blotting. The membranes were probed with an antibody recognizing the N-terminal fragment (BR5) of SBP1.

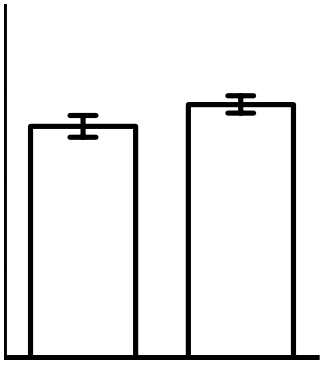

Fig. S6. Binding of 3D7 parent parasites to CD36 under flow conditions. Control (0 mM) or GlcN-treated (2.5 mM) infected RBCs (3% parasitemia, 1% hematocrit) were flowed at 0.1 Pa over recombinant CD36. The number of bound infected RBCs was counted. P = 0.125, unpaired t-test. Error bars represent the S.E.M. of data collected in 3 separate experiments (10 fields each experiment).

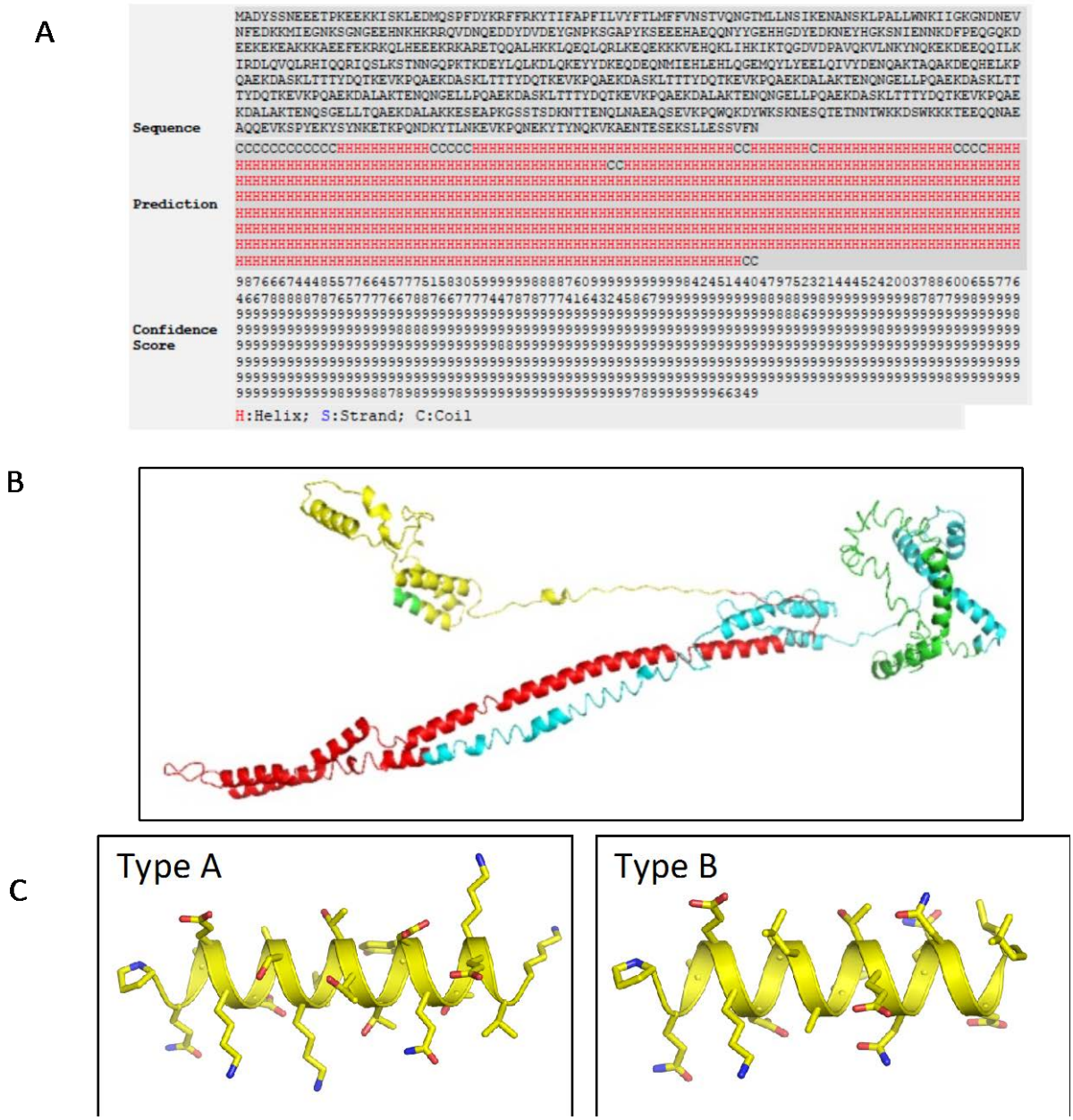

Fig. S7. I-TASSER prediction of REX1 protein structure. A. Prediction of REX1 secondary structure with confidence scores. B. Top model predicted for REX1 protein structure is based on Tc toxin from bacteria, a protein involved in host membrane perforation (1vw1A). C. Repeat sequences were constructed as ideal α-helices. Type A repeats have two pairs of lysine residues and a glutamate/aspartate pair, in which like-charged side chains occupy adjacent positions in the structure. Type B repeats contain more negatively charged amino acids, which are distributed over the surface of the helix.

Video S1. Rendered 3D model of a Maurer's cleft stack (green) from a REX1$^{(\Delta 371–579)}$-GFP parasite imaged by STEM tomography (600 nm section). The infected RBC was fixed in paraformaldehyde/glutaraldehyde, permeabilized with EqtII and labelled with anti-GFP and Protein A gold (yellow). Tether-like structures extending from the clefts are rendered in magenta.

Video S2. Live cell microscopy of ring stage REX1-GFP parasites showing mobile Maurer's clefts.

Video S3. Live cell microscopy of ring stage REX1$^{(\Delta 371–579)}$-GFP parasites showing Maurer's clefts with limited mobility.

Video S4. Live cell microscopy of ring stage REX1$^{(\Delta 371–579)}$-GFP parasites showing mobile Maurer's clefts.